Simulation and Optimization of Flow Patterns in an Oscillatory Central Baffled Reactor: Enhancing Mixing and Energy

Safaa M. R. Ahmed
Chemical Engineering Department, College of Engineering, Tikrit University, Salah al-Din, Iraq
cssuiq@gmail.com

Mudheher M. Ali
Chemical Engineering Department, College of Engineering, Tikrit University, Salah al-Din, Iraq
Adnan82114@gmail.com

Saba A. Gheni
Chemical Engineering Department, College of Engineering, Tikrit University, Salah al-Din, Iraq
ghenis@tu.edu.iq (corresponding author)

Received: 19 July 2024 | Revised: 6 August 2024 | Accepted: 11 August 2024

 DOI: https://doi.org/10.48084/etasr.8441

ABSTRACT

This research analyses the flow patterns in an Oscillatory Central Baffled Reactor (OCBR) using Computational Fluid Dynamics (CFD) simulations under various oscillation conditions. Frequency (f) and amplitude (x_0) are examined as critical parameters for enhancing fluid mixing and energy efficiency in high viscosity fluids, such as biofuels. The findings highlight the significant impact of the Strouhal number (St) on the flow behavior, showing improved fluid mixing with an increase in the oscillatory Reynolds number (Re_0) from 125.6 (f = 2 Hz, x_0 = 2 mm) to 392.7 (f = 2.5 Hz, x_0 = 5 mm), corresponding to a decrease in the St from 0.2 to 0.08. The simulations indicated the appearance of stable vortices and a better distribution of the Weibel dead zones at an oscillation cycle (t/T) of 0.5. During the course of the study, the pressure distribution within the OCBR and its dependence on oscillation amplitude were shown, which significantly impacted the pressure drop from 8.8 to 123 Pa as Re_0 was raised. In order to alleviate the endpoints for high resistance of sharp edged baffles, two modified baffle designs (semi-central and smooth-edge central baffles) were used. The findings showed that the performance of the semi-central baffle design in terms of dead zone reduction and shear stress was superior to those of the other designs for both upward and downward flows, indicating its suitability for enhancing the performance of the OCBR. This research offers important developments in the efficient mixing processes needed in industrial applications and indicates some areas for effective testing and validation of the models developed.

Keywords-Oscillatory Central Baffled Reactor (OCBR); Computational Fluid Dynamics (CFD); Strouhal number; Reynolds number; central baffle; flow pattern; simulation; pressure distribution

I. INTRODUCTION

Due to their improved mixing and mass transfer capabilities compared with conventional reactors, the Oscillatory Baffled Reactors (OBRs) have received a great deal of attention in recent years. In those, mixing is simply done by the flow and in some devices with a little periodic stroke to get better processes [1, 2]. The stirring leads to the wagging motion of these reactors, which complicates mixing so much that it affects reaction rate and product distribution. Central baffled designs particularly have strived to enhance these flow behaviors by abrupt placement on baffles across the laminar flow stream to induce turbulence [1, 3]. The potential of the OBRs has been showcased in different applications in the most recent developments. For example, in [4], the use of OBRs improved the mass transfer rates in the biochemical processes, which consequently led to increased product yield. According to [5], such OBRs performed experiments and reported benefits of improved mixing and energy savings over stirred tank reactors. Baffles are internal features that create controlled recirculating flows and authors in [6] modeled their shape in order to understand how they affect the flow patterns and indicated that certain baffle designs can be used to enhance mixing and reduce dead zones in the reactor. Authors in [7] showed that mixing is also improved for baffled tubes with oscillatory flow. Authors in [8] stressed the right compatibilization of OBRs for continuous processing operations. Authors in [9] focused on

the effects of the oscillatory flow over baffle geometry within a continuous reactor and concluded that proper baffle geometry might be able to boost mass transfer further. In [10], detailed numerical simulations of the flow inside an OBR by advanced CFD techniques were conducted and the oscillation on the mixing performance and residence time distribution was discussed. However, still several aspects of these recent advances leave some aspects for improvement to cover the existing gaps with respect to OBRs, particularly on how flow behaves in Oscillatory Central Baffled Reactor (OCBR) systems as well as design configuration challenges. The majority of studies focused on bifurcations of the types of baffle-and-pipe configurations, orifice and helical designs [11-13], but have not examined the influence of oscillation parameters (frequency and amplitude) and baffle arrangements on hydrodynamics and mixing efficiency.

A limitation of this review is the absence of full-system simulation studies that could have used experimental data to demonstrate findings. Although many studies have been conducted on the flow dynamics and mixing performance characteristics [2, 3] of some helical mixers impellers in an oscillatory regime [4], they very rarely focus on the detailed effect of moving central baffles which also play important role. Therefore, this work is an attempt to provide data about the flow patterns inside OCBR through CFD simulations. We consider subjects such as how oscillation frequency and amplitude affect mixing intensity for different models through simulation by isolating baffle configurations to study flow increase and specific baffle mixing. We also investigate other avenues in reactor design for possible improvements. The principal objectives of this study are to determine and quantify the flow patterns in an OCBR for different operating conditions using CFD to characterize mass transfer within the reactor and optimize it, if possible and suggest design modifications on account based model simulation results that would assist optimizing reactor performance. This study will not only advance fundamental comprehension about the hydrodynamics of OCBRs, but also contribute to optimize reactor design and operation. Results from this study will inform the design of better, large scale OCBRs suitable for a variety range of chemical processes.

II. THEORY OF OSCILLATORY FLOW

A. Equations

The flow pattern in OBRs is governed by three dimensionless groups. These are:

The net flow Reynolds number which determines the net flow:

$$\mathrm{Re}_n = \frac{\rho \cdot v_0 \cdot D}{\mu} \quad (1)$$

where ρ is the liquid density (kg/m^3), v_0 is the net flow velocity (m/s), D is the reactor diameter (m), and μ is the liquid viscosity (Pa·s or kg/(m·s)).

The oscillatory Reynolds number (Re_o), is defined by (2) and determines the oscillation intensity:

$$\mathrm{Re}_0 = \frac{2\pi \cdot f \cdot x_0 \cdot \rho \cdot D}{\mu} \quad (2)$$

where f is the oscillation frequency (Hz or cycles/s) and x_0 is the oscillation amplitude (m).

The Strouhal number (St), is defined by (3) and determines the eddy propagation:

$$St = \frac{D}{4\pi \cdot x_0} \quad (3)$$

B. Flow Visualization – Numerical Simulations

The current study examined the geometry of the oscillatory central baffled reactor shown in Figure 1a. The diameter of the ball was 5 mm, while the diameter of the central baffle was 3.5 mm, and the distance between baffles was 7.5 mm. In terms of dimensions, the opening cross section area, S, is 0.49. The total length of the field was 25 mm and included 3 central baffles. To suppress the numerical errors at the point of contact with the baffling tube wall, a small portion of the mesh was cut (Figure 1b). A uniformly organized 3D hexagonal mesh was created in COMSOL Multiphysics 5.4. The mesh contains 19,902 boundary elements and 976 edge elements, giving a total number of 251,929 cells.

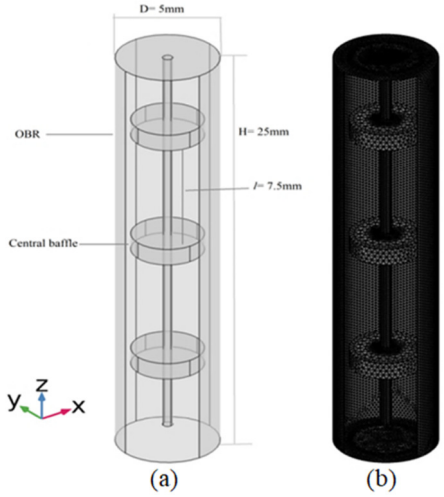

Fig. 1. (a) 3D scheme of OBR, (b) 3D surface mesh.

C. Model Configuration and Boundary Conditions

The laminar analyzer was chosen for this study using water (density: 998.2 kg/m^3 and viscosity: 0.0010 Pa·s) as the working fluid. Here, the standard continuity (4) and Navier - Stokes (5) equations for determining the incompressible flow are used:

$$\frac{\partial(v_i)}{\partial x_i} = 0 \quad (4)$$

where v_i is the velocity (m/s) vector and x_i the amplitude (m) in each dimension.

$$\frac{\partial(v_i)}{\partial \mathrm{t}} + \frac{\partial(v_i v_j)}{\partial x_j} = -\frac{1}{\rho}\frac{\partial P}{\partial x_i} + \frac{\mu}{\rho}\frac{\partial}{\partial x_j}\left(\frac{\partial(v_i)}{\partial x_j}\right) \quad (5)$$

where P is the pressure (N/m^2) field and t the time (s).

The inlet fluid velocity consists of both net and oscillatory components. It is defined by:

$$v(\mathrm{t}) = v_0 + 2\pi \cdot f \cdot x_0 \cdot \sin\left(2\pi \cdot f \cdot \mathrm{t}\right) \quad (6)$$

where v_0 is the net flow velocity (determined from $\mathrm{Re_n}$), and f, x_0 are the oscillations frequency and amplitude respectively (specified from $\mathrm{Re_0}$). The time interval was 50 time steps per oscillation cycle. The actual time steps used are evidenced in Table I. The simulation was run for 25 complete oscillation cycles to ensure that the results can be considered independent of the initial conditions.

TABLE I. OSCILLATION CONDITIONS WITH TIME STEPS

Run	$\mathrm{Re_0}$	x_0, (mm)	St	f, (Hz)	Δt, (ms)
1	125.6	2	0.2	2	12
2	125.6	4	0.1	1	3
3	392.7	5	0.08	2.5	2.5

The velocity fields in 8 phases of the oscillation cycle, corresponding to the points of maximum acceleration/deceleration, maximum velocity, and flow reversal were compared, as illustrated in Figure 2. To reduce the experimental noise, the flow patterns in each of these 8 oscillation cycles were phase-averaged over 15 oscillation cycles.

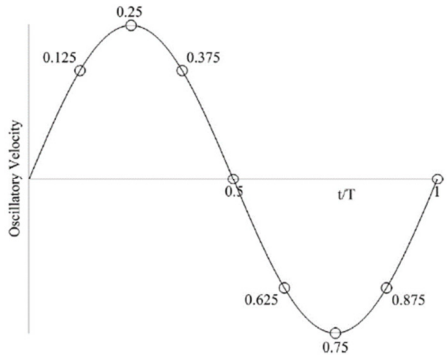

Fig. 2. Oscillatory velocity and cycle phases.

III. RESULTS AND DISCUSSION

A. 2D Velocity Fields

Figures 3-5 present the simulation results of the velocity magnitude and flow patterns at different Oscillation Conditions (OC) and time steps. Each sub-image represents the evolution of the flow at specific times in terms of the oscillation cycle: t/T = 0.125, 0.250, 0.375, and 0.5. The 2D velocity fields (Figures 3-5) reveal a significant evolution of the flow in the OCBR over the oscillation cycle. At the initial phase (t/T = 0.125), the flow appears primarily unidirectional with high velocities near the channel edges, indicating sharp velocity gradients and potential regions of poor mixing. As the oscillation cycle progresses (t/T = 0.25 and t/T = 0.375), complex flow patterns and recirculation zones begin to form near the baffle regions. By the final phase (t/T = 0.5), the flow pattern is well-developed with prominent vortices, particularly in the higher frequency and amplitude conditions (Figure 5). These vortices are indicative of enhanced mixing and energy dissipation, crucial for improving reaction efficiency in the OCBR. The observed evolution of the flow patterns suggests that higher oscillation frequencies and amplitudes lead to more vigorous mixing and reduced axial dispersion. This finding aligns with previous studies, such as [8, 9], which reported improved mixing and mass transfer rates with increased oscillatory intensity.

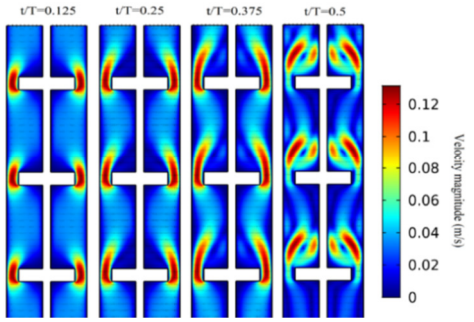

Fig. 3. Velocity evolution - OC: $\mathrm{Re_n}$ = 0, $\mathrm{Re_0}$ = 125.6, St = 0.2, (x_0 = 2 mm, f = 2 Hz).

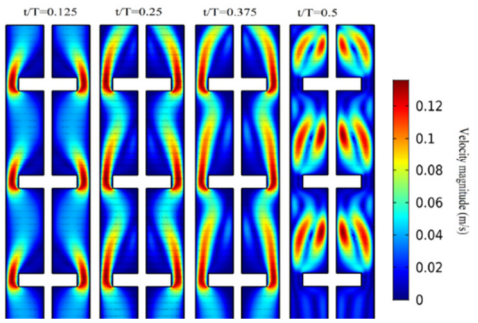

Fig. 4. Velocity evolution - OC: $\mathrm{Re_n}$ = 0, $\mathrm{Re_0}$ = 125.6, St = 0.1, (x_0 = 4 mm, f = 1 Hz).

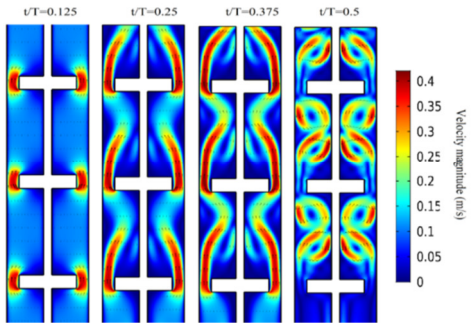

Fig. 5. Velocity evolution - OC: $\mathrm{Re_n}$ = 0, $\mathrm{Re_0}$ = 392.76, St = 0.08, (x_0 = 5 mm, f = 2.5 Hz).

In Figures 3-5, dead areas or poor mixing are observed in some OCBR regions at oscillation cycles t/T = 0.125, 0.250, 0.375. However, at the last time step, the mixing becomes uniform due to increased recirculation and vortex formation, especially in Figure 5 (f = 2.5 Hz and x_0 = 5 mm), where four vortices are generated in each baffle cell, unlike Figures 3 and 4, where only two vortices appear. This baffle design has specific benefits, including providing high shear at the baffle

edges for mixing high-viscosity fluids and increasing heat and mass transfer by trapping fluid under the baffles, resulting in an increased transmission surface area. It can be concluded that the baffle design is very sensitive to the oscillation conditions, particularly amplitude, as the flow pattern improves with increased oscillation conditions. Therefore, the arrangement of a good flow pattern, including velocity distribution, number of vortices, and their size, can be as follows: Figure 5 (5 mm and 2.5 Hz) > Figure 4 (4 mm and 1 Hz) > Figure 3 (2 mm and 2 Hz). The flow patterns of the down flow (t/T = 0.625, 0.75, 0.875, and 1) are similar to those in Figures 3-5 but in the opposite direction.

B. Pressure Distribution

Figures 6-8 show contours of the pressure distribution within the OCBR for up-flow and down-flow directions, where high-pressure zones are presented in red and low-pressure zones in blue. In general, the pressure in OBRs varies from negative to positive based on the flow direction due to the specific flow mechanism found in OBRs. The oscillatory flow involves the up and down movement of the fluid, creating areas of alternating high and low pressure due to inertial and frictional forces acting on the fluid. Negative pressure (Figures 6(a), 7(a), 8(a)) occurs when the fluid moves upward, generating a temporary low-pressure region below the central baffle. Positive pressure (Figures 6(b), 7(b), 8(b)) occurs during downward flow due to high back pressure and gravity.

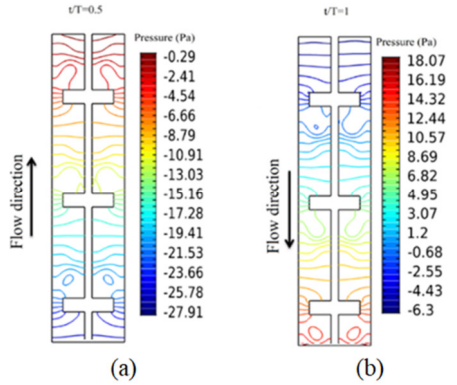

Fig. 6. Pressure contours: (a) up-flow, (b) down-flow - OC: $Re_n = 0$, $Re_0 = 125.6$, St = 0.2, ($x_0 = 2$ mm, $f = 2$ Hz).

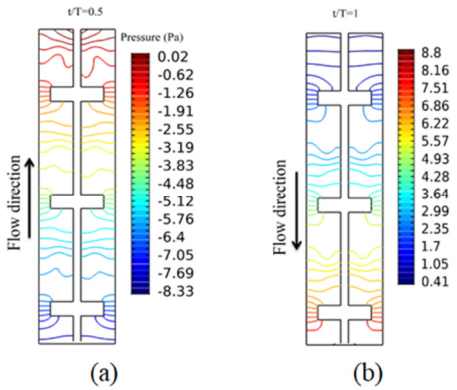

Fig. 7. Pressure contours: (a) up-flow, (b) down-flow - OC: $Re_n = 0$, $Re_0 = 125.6$, St = 0.1, ($x_0 = 4$ mm, $f = 1$ Hz).

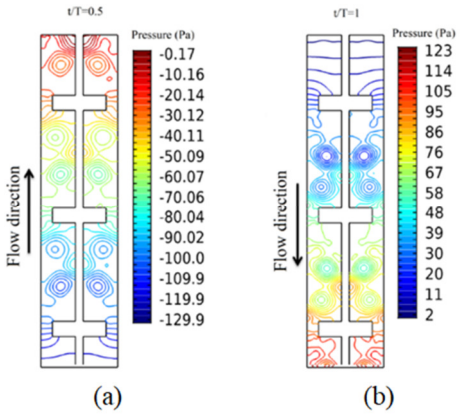

Fig. 8. Pressure contours: (a) up-flow, (b) down-flow - OC: $Re_n = 0$, $Re_0 = 392.76$, St = 0.08, ($x_0 = 5$ mm, $f = 2.5$ Hz).

Figure 8 displays a lower pressure value (-129 Pa) during the downward flow and a higher pressure value (123 Pa) during the upward flow compared to the other conditions (Figures 6 and 7). The pressure distribution within the OCBR varies significantly between the upward and downward phases of the oscillation cycle. High-pressure zones are observed near the baffles during the upward flow, while low-pressure zones dominate during the downward flow. The pressure differential is most pronounced in the high oscillatory Reynolds number condition (Re_0 = 392.76, Figure 8), indicating that higher oscillation intensities result in greater pressure variations and, consequently, more effective mixing. The pressure drop across the baffles, as observed in the high-frequency and amplitude conditions, stresses the increased energy requirements for achieving enhanced mixing. However, this trade-off is justified by significant improvements in mixing efficiency and mass transfer rates, which are essential for optimizing the performance of OCBRs in chemical processes.

C. Modification of Baffle Design

The study also explores the impact of modified baffle designs (Figure 9) on flow patterns and pressure distribution.

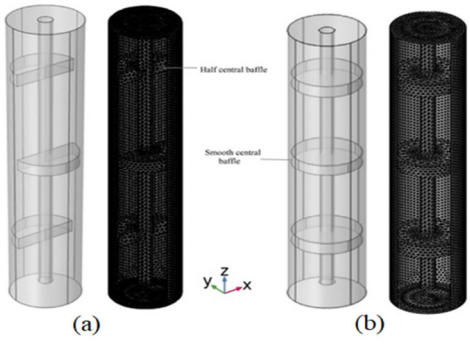

Fig. 9. Modified OBRs: (a) semi-central baffle design, (b) smooth-edge central baffle design.

To reduce the resistance of the sharp-edged central baffle to the oscillatory flow, two new baffle designs were suggested: semi-central baffle design (Figure 9(a)) and smooth-edge central baffle design (Figure 9(b)). In the semi-central design,

the baffles extend only partially across the reactor, generating a unique flow pattern compared to a full central baffle design. In the smooth-edge design, the fluid flows smoothly around the baffle with little resistance compared to the sharp design.

1) 2D Velocity Fields

Figure 10 showcases the flow patterns in the modified OCBRs and their comparison with the sharp-edge central design at oscillation conditions: Re_n = 0, Re_0 = 392.76, St = 0.08 (x_0 = 5 mm, f = 2.5 Hz).

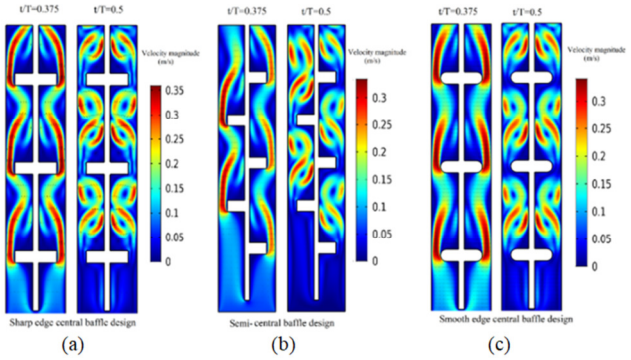

Fig. 10. Velocity comparing: (a) sharp edge central baffle, (b) semi-central baffle, (c) smooth edge central baffle.

2) Pressure Distribution

Figures 11 and 12 show contours of pressure in the three designs, at oscillation conditions: Re_n = 0, Re_0 = 392.76, St = 0.08 (x_0 = 5 mm, f = 2.5 Hz).

During the upward flow (Figure 11), the sharp-edge central baffle exhibits a significant pressure build-up (-130 Pa) as the fluid encounters the obstruction, while it is lower in the semi-centric baffle (-95 Pa) and slow in the smooth central design (-110 Pa). At the downward flow (Figure 12), the central design with sharp edges causes a sharp pressure drop (ΔP = 120 Pa) due to flow separation and the formation of wake zones. However, it is less steep in the semi-central design (ΔP = 100 Pa) and more gradual in the smooth-edge design (ΔP = 112 Pa). Researchers in [14, 15] found out that the pressure drops in different designs of OBRs. For example, in the donut and disc designs, it is approximately 150 Pa. The observed improvements in the flow patterns and pressure distributions with modified baffle designs are consistent with the findings in previous studies. For instance, in [10], it is demonstrated that altering baffle geometries can significantly enhance the mixing efficiency in oscillatory reactors. Similarly, in [11], it is shown that modified baffle designs could reduce dead zones and improve the overall reactor performance. The present study corroborates these findings by displaying that both semi-central and smooth-edge baffle designs lead to better fluid dynamics and reduced pressure drops, ultimately enhancing mixing and energy efficiency in OCBRs. Future research could explore the optimization of baffle geometries for specific industrial applications, such as pharmaceutical production or wastewater treatment, where efficient mixing and mass transfer are critical. Additionally, integrating CFD simulations with experimental validation can provide deeper insights into the complex flow behaviors in OCBRs. Potential applications of these findings include the design of more efficient reactors for chemical synthesis, biofuel production, and other processes requiring precise control over mixing and reaction conditions.

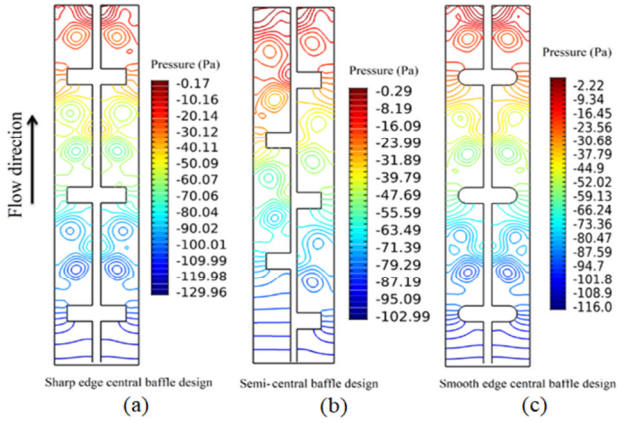

Fig. 11. Up-flow pressure contours: (a) sharp edge central baffle, (b) semi-central baffle, (c) smooth edge central baffle.

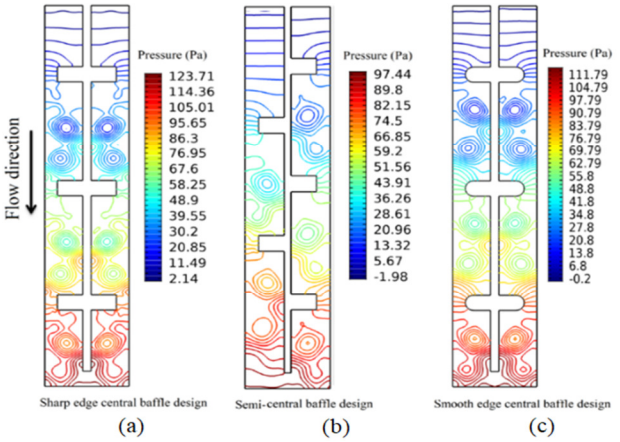

Fig. 12. Down-flow pressure contours: (a) sharp edge central baffle, (b) semi-central baffle, (c) smooth edge central baffle.

IV. CONCLUSIONS

The results of the CFD study help us understand the OCBRs in a more detailed fashion. It was showed through CFD analysis that OCBR's mixing and mass-transfer efficiency improves with oscillation frequencies of up to 2.5 Hz and oscillation amplitudes of up to 5 mm, although sharp-edge central baffles give rise to pressure heads swinging between -130 Pa to 120 Pa. Rather, the smooth-edge baffles obtain these pressure areas without dropping off efficiency. Further, baffles such as semi-central baffle which are designed without activators improve the flow dynamics while they decrease the energy requirements. This information can serve on the implementation of practical steps on how to best design and operate OCBR's that are more effective and easily scalable for use in different chemical processes. Creation of the modified baffle designs and improved mixing systems would most probably require less energy than conventional methods of baffle arrangement. This speaks of the necessity of design of

baffles in relation to the process conditions. Such results advance the knowledge of OCBR operation and suggest solutions to the OCBR reactor modification and operation for higher efficiency and scalability.

REFERENCES

[1] A. N. Phan and A. Harvey, "Development and evaluation of novel designs of continuous mesoscale oscillatory baffled reactors," *Chemical Engineering Journal*, vol. 159, no. 1, pp. 212–219, May 2010, https://doi.org/10.1016/j.cej.2010.02.059.

[2] J. R. McDonough, A. N. Phan, and A. P. Harvey, "Rapid process development using oscillatory baffled mesoreactors – A state-of-the-art review," *Chemical Engineering Journal*, vol. 265, pp. 110–121, Apr. 2015, https://doi.org/10.1016/j.cej.2014.10.113.

[3] A. N. Phan and A. P. Harvey, "Effect of geometrical parameters on fluid mixing in novel mesoscale oscillatory helical baffled designs," *Chemical Engineering Journal*, vol. 169, no. 1, pp. 339–347, May 2011, https://doi.org/10.1016/j.cej.2011.03.026.

[4] N. Reis, A. A. Vicente, J. A. Teixeira, and M. R. Mackley, "Residence times and mixing of a novel continuous oscillatory flow screening reactor," *Chemical Engineering Science*, vol. 59, no. 22, pp. 4967–4974, Nov. 2004, https://doi.org/10.1016/j.ces.2004.09.013.

[5] M. R. Mackley and X. Ni, "Experimental fluid dispersion measurements in periodic baffled tube arrays," *Chemical Engineering Science*, vol. 48, no. 18, pp. 3293–3305, Sep. 1993, https://doi.org/10.1016/0009-2509(93)80213-A.

[6] X.-W. Ni, A. Fitch, and H. Jian, "Numerical and Experimental Investigations into The Effect of Gap Between Baffle and Wall on Mixing in an Oscillatory Baffled Column," *International Journal of Chemical Reactor Engineering*, vol. 2, no. 1, Sep. 2004, https://doi.org/10.2202/1542-6580.1147.

[7] P. Stonestreet and P. M. J. Van Der Veeken, "The Effects of Oscillatory Flow and Bulk Flow Components on Residence Time Distribution in Baffled Tube Reactors," *Chemical Engineering Research and Design*, vol. 77, no. 8, pp. 671–684, Nov. 1999, https://doi.org/10.1205/026387699526809.

[8] M. R. Hewgill, M. R. Mackley, A. B. Pandit, and S. S. Pannu, "Enhancement of gas-liquid mass transfer using oscillatory flow in a baffled tube," *Chemical Engineering Science*, vol. 48, no. 4, pp. 799–809, Feb. 1993, https://doi.org/10.1016/0009-2509(93)80145-G.

[9] P. Gough, X. Ni, and K. C. Symes, "Experimental Flow Visualisation in a Modified Pulsed Baffled Reactor," *Journal of Chemical Technology & Biotechnology*, vol. 69, no. 3, pp. 321–328, 1997, https://doi.org/10.1002/(SICI)1097-4660(199707)69:3<321::AID-JCTB717>3.0.CO;2-Q.

[10] M. Zheng *et al.*, "Characterization of macromixing and micromixing performance of unbaffled U-shaped mesoscale oscillatory flow reactor," *Journal of the Taiwan Institute of Chemical Engineers*, vol. 145, Apr. 2023, Art. no. 104852, https://doi.org/10.1016/j.jtice.2023.104852.

[11] A. García, J. P. Solano, P. G. Vicente, and A. Viedma, "Flow pattern assessment in tubes with wire coil inserts in laminar and transition regimes," *International Journal of Heat and Fluid Flow*, vol. 28, no. 3, pp. 516–525, Jun. 2007, https://doi.org/10.1016/j.ijheatfluidflow.2006.07.001.

[12] H. Jian and X. Ni, "A Numerical Study on the Scale-Up Behaviour in Oscillatory Baffled Columns," *Chemical Engineering Research and Design*, vol. 83, no. 10, pp. 1163–1170, Oct. 2005, https://doi.org/10.1205/cherd.03312.

[13] J. R. McDonough, S. M. R. Ahmed, A. N. Phan, and A. P. Harvey, "A study of the flow structures generated by oscillating flows in a helical baffled tube," *Chemical Engineering Science*, vol. 171, pp. 160–178, Nov. 2017, https://doi.org/10.1016/j.ces.2017.05.032.

[14] A. Mazubert, D. F. Fletcher, M. Poux, and J. Aubin, "Hydrodynamics and mixing in continuous oscillatory flow reactors—Part I: Effect of baffle geometry," *Chemical Engineering and Processing: Process Intensification*, vol. 108, pp. 78–92, Oct. 2016, https://doi.org/10.1016/j.cep.2016.07.015.

[15] T. P. Minh *et al.*, "Finite Element Modeling of Shunt Reactors Used in High Voltage Power Systems," *Engineering, Technology & Applied Science Research*, vol. 11, no. 4, pp. 7411–7416, Aug. 2021, https://doi.org/10.48084/etasr.4271.